Journal of Drug Delivery Science and Technology 99 (2024) 105974

Contents lists available at ScienceDirect

Journal of Drug Delivery Science and Technology

journal homepage: www.elsevier.com/locate/jddst

Microbeads produced by prilling/vibration technique: A new way to use polyvinyl alcohol in pediatric and veterinary formulations

Marianna Ivone [a], Nunzio Denora [a], Vita D'Amico [a], Lena Mareczek [b], Lena Karin Mueller [b], Ilaria Arduino [a], Alessandra Ambruosi [b], Angela Assunta Lopedota [a,*]

[a] Department of Pharmacy-Pharmaceutical Sciences, University of Bari Aldo Moro, 4 E. Orabona, street, 70125, Bari, Italy
[b] Merck Life Science KGaA, Frankfurter Straße 250, 64293, Darmstadt, Germany

ARTICLE INFO

Keywords:
Poly(vinyl alcohol)
Ibuprofen
Ketoconazole
Prilling/vibration technique
Drug delivery systems

ABSTRACT

Poly(vinyl alcohol) (PVA) is a widely used synthetic polymer and due to its hydrophilicity, biocompatibility, and biodegradability, it is considered a suitable polymer for the formulation of drug delivery systems. In this study, PVA was used in a prilling/vibration technology as a pharmaceutical grade excipient to produce microbeads for oral administration that improve class II drugs' solubility and dissolution rate according to the Biopharmaceutical Classification System (BCS). Specifically, Ibuprofen (IBU) is a weakly acidic drug with low solubility at pH 1.2 and Ketoconazole (KETO), a weakly basic drug characterized by low solubility at pH 6.8. These drugs were selected because of their requirements for specific dosing conditions in children or animals, which often differ from commercially available conventional drugs. The microbeads produced were fully characterized in terms of drug loading, encapsulation efficiency, size, morphology, and drug release experiments were also conducted in a gastric fluid for IBU-loaded microbeads and simulated intestinal fluid for KETO-loaded microbeads. Finally, PVA microbeads were compared with an amorphous solid dispersion (ASDs) of the respective APIs, showing the same increase in solubility and dissolution rate. Therefore, the use of the prilling/vibration technology to produce PVA-based microbeads containing BCS class II drugs improves solubility and dissolution profile, which represent fundamental requirements for good bioavailability. Furthermore, the manufactured microbeads provide a high degree of dosing flexibility, making them suitable for administration in pediatric or veterinary patients with swallowing difficulties and requiring customized dosing.

1. Introduction

Poly(vinyl alcohol) (PVA) represents a fascinating milestone in polymer science, offering various applications in various fields, from industry to biomedical engineering. PVA is one of the hydrophilic biodegradable synthetic polymers obtained by polymerization of the vinyl acetate monomer into polyvinyl acetate (PVAc), followed by a partial hydrolysis of the acetate groups to obtain PVA. This synthetic polymer, which is characterized by its water-solubility and biodegradability, has attracted great attention due to its exceptional properties and versatility in various fields, such as the biomedical and pharmaceutical sectors, due to its compatibility, safety, good hydrogel formation and high swelling properties [1–3]. Additionally, it is frequently employed as an excipient in oral pharmaceutical formulations, to enhance the solubility of drugs including those designed for pediatric administration, due to its biocompatibility, minimal toxicity, and inert nature [4,5].

Among the oral formulations dedicated to pediatric and veterinary use, multi-particulates (microcapsules and microbeads) are gaining particular attention due to their flexibility in dosing to meet the unique needs of subjects with varying weights, including those in the growth and development phase. This adaptability is particularly advantageous in populations where weight discrepancies are common, such as children versus adults [6]. Conventional drug formulations have limitations when administered to pediatric patients because they were not designed for this patient population. As a result, manipulation and compounding have become common practices. Multi-particulates, on the other hand, offer dosing flexibility and small size that facilitate administration, increase acceptability, and improve compliance [7]. Multi-particulates offer better patient acceptability than single-unit solid pharmaceutical forms (e.g. tablets and capsules) as they can be administered directly into the patient's mouth, sprinkled in appropriate baby food, dispersed

* Corresponding author.
E-mail address: angelaassunta.lopedota@uniba.it (A.A. Lopedota).

https://doi.org/10.1016/j.jddst.2024.105974
Received 15 May 2024; Received in revised form 3 July 2024; Accepted 12 July 2024
Available online 14 July 2024

in suitable foodstuffs, swallowed directly using a dose-measuring device such as a dosing spoon or dosing sipping technology or successfully inserted into capsules [8,9]. Similarly, multi-particulate formulations tailored for veterinary use offer several advantages over single-unit dosage forms, providing enhanced flexibility in dosing and administration, precise adjustment of dosage based on the animal's size, weight, and species, improved palatability, ease of mixing with feed, and minimize the risk of incomplete ingestion or 'dose dumping' [10].

To demonstrate the applicability of multi-particulates as formulations for pediatric and veterinary use, two classic drugs, Ibuprofen (IBU) and Ketoconazole (KETO), were studied. These drugs were selected because of their requirements for specific dosing conditions in children or animals, which often differ from commercially available conventional drugs. In addition, these two drugs present solubility problems, in fact they are classified in class II according to the Biopharmaceutical Classification System (BCS). In particular, IBU is a weakly acidic drug with a low solubility at pH 1.2 (0.023 mg/mL) and a higher solubility at pH 6.8 (3.37 mg/mL) [11], while KETO is a weakly basic drug characterized by a low solubility at pH 6.8 (0.003 mg/mL) and a higher solubility at pH 1.2 (20 mg/mL) [12]. IBU is a widely known compound of non-steroidal anti-inflammatory drugs. It is mostly used as a relieving agent in acute and chronic pain and inflammation [13]. Different oral suspensions are commercially available for pediatric use however, there are not solid pharmaceutical forms that can meet the different therapeutic dosages required by this population group [14,15].

KETO is an azole fungistatic medication commonly used in veterinary medicine to treat various fungal infections in dogs and cats and as an extra-label drug in various species [16].

Starting from this premise, the idea of this work is to realize PVA-microbeads loaded IBU or KETO by prilling/vibration technique capable to improve the solubility and dissolution rate of the respective drugs for a specific application field (pediatric or veterinary). Among different physical methods for microencapsulation such as the well-known spray drying, fluid bed coating, extrusion, etc. [17], an innovative technique known as prilling/vibration technology is able to produce microcapsules or microbeads with a very narrow dimensional range and high encapsulation efficiency [18]. The technique is based on breaking a laminar jet of polymer solution into a line of one-dimensional droplets using a vibrating nozzle device. The resulting droplets fall into a consolidation bath and are solidified as microbeads [19–21]. The microbeads produced were completely characterized in terms of drug loading, encapsulation efficiency, size, and morphology. Drug release experiments were also conducted in a simulated gastric or intestinal fluid. Finally, the PVA microbeads were compared to another technological approach, the amorphous solid dispersions (ASD), to evaluate whether the new microbead formulations produced the same advantage in terms of solubility and dissolution rate.

2. Materials and methods

2.1. Materials

Poly(vinyl alcohol) 3–82 (Parteck® MXP) was kindly provided by Merck KGaA (Darmstadt, Germany). The grade of PVA has two groups of numbers separated by a hyphen therefore it is appropriate to explain this nomenclature. The first group of numbers represents the viscosity of the 4 % w/v aqueous solution at 20 °C. The second group of numbers represents the degree of hydrolysis of the PVAc. Thus, a grade 3–82 would have a viscosity of 3 mPa s in a 4 % w/v aqueous solution at 20 °C with a polymer chain consisting of approximately 82 % PVA and 18 % PVAc. Alginic acid sodium salt (MW = 120,000–190,000 g/mol, with a mannuronic acid to ratio of 1.56, viscosity of solution at 1 % w/v at 25 °C = 15–25 cps), boric acid (H_3BO_3), calcium chloride ($CaCl_2$), and potassium bromide (KBr) were purchased from Sigma-Aldrich (Milan, Italy). IBU and KETO were obtained from Farmalabor srl, (Canosa di Puglia, Italy). All solvents and salts used were of analytical grade and were acquired from Sigma Aldrich (Milan, Italy).

2.2. Preparation of microbeads by prilling/vibration technique

2.2.1. Feed preparation

Solutions of PVA 3–82 were utilized to prepare the polymeric feed. The PVAs were dispersed in water and the suspensions were heated above 90 °C for 5 min, then the solutions were left to cool to room temperature under agitation to eliminate bubbles formed. Viscosity of 6, 9, and 20 % w/v solutions of PVA 3–82 was evaluated by Haake Mars Rheo 60 (Thermo Fisher Scientific, USA - MA). Furthermore, solutions at 20 % w/v of PVA 3–82 and sodium alginate (SA) were produced in which the weight ratios of the two polymers were varied (100:0, 100:1, 71:1, 50:1, 33:1, 25:1, 19:1) i.e., S_0, S_1, S_2, S_3, S_4, S_5 and S_6 respectively (Table 2).

2.2.2. Selection of process parameters

The microbeads were obtained by the prilling/vibration technique using the B395 Pro Encapsulator (Büchi Labortechnik AG, Flawil, Switzerland). The different feeds (Table 1) were pumped using a syringe pump through a single nozzle with a diameter of 450 μm. Other process parameters were carefully optimized to obtain well-separated and spherical microbeads. The laminar jet of the liquid was broken up using a vibration frequency of 1000 Hz, which determined the number and the size of droplets. The electrode potential was set at 1200 V to avoid droplet coalescence and the distance between the nozzle and the consolidation bath was set at 20 cm. A volumetric flow rate of about 10 mL/min and an amplitude of 8 were used. The droplets generated by each polymer feed were gelled under gentle agitation for 10 min at room temperature in two different gelling baths of aqueous solution (300 mL) with:

a) $CaCl_2$ 0.3 M (a-bath);
b) $CaCl_2$ 0.18 M and H_3BO_3 0.4 M (b-bath).

Then, microbeads were recovered and thoroughly rinsed twice with deionized water to remove excess calcium and H_3BO_3 on the surface of the microbeads. Finally, microbeads were frozen at −20 °C and freeze-dried using a Christ Alpha 1–4 under reduced pressure (0.018 mbar) at −50 °C for 24 h.

In the same way, the best-performant feed (S_6) was loaded with 0.15 % w/v IBU or KETO, resulting in four formulations called F_{6a}IBU, F_{6a}KETO, F_{6b}IBU, and F_{6b}KETO where the subscripts a and b indicate the different consolidation bath used. In addition, in the F_{6b}IBU formulation, the amount of drug was further increased 4 (0.6 % w/v) and 14-fold (2.1 % w/v).

2.3. Preparation of amorphous solid dispersion loading ibuprofen or ketoconazole

PVA-amorphous solid dispersions (PVA-ASDs) loading IBU or KETO were produced according to the solvent evaporation method [22]. Solid polymer-drug mixtures 20 % PVA 3–82 and 0.15 % w/v IBU or KETO were solubilized in ethanol-water (50:50 v/v) to produce the ASD-IBU

Table 1
Polymeric feeds composition (100 mL) that produced aqueous solutions at pH 6.5.

Feed code	PVA 3–82 (% w/v)	SA (% w/v)	Ratio PVA 3–82:SA
S_0	20.0	0.0	100:0
S_1	19.8	0.2	100:1
S_2	19.7	0.3	71:1
S_3	19.6	0.4	50:1
S_4	19.4	0.6	33:1
S_5	19.2	0.8	25:1
S_6	19.0	1.0	19:1

Table 2
Yield %, and size of the dried microbeads placebo. Data are reported as the mean ± SD.

Formulation Code	Yield %	Diameter microbeads (μm)
F_{6a}	45.31 ± 3.74	1605 ± 185
F_{6b}	70.01 ± 2.06	2050 ± 207

and ASD-KETO formulations. Then, the solvent was removed using Rotavapor R-200 Büchi (Flawil, Switzerland) (at 55 °C, 20 mbar), and a vitreous powder was formed on the surfaces of the flask. Subsequently, the powder was collected from the surface of the flask and sieved using a 355 μm sieve to ensure dimensional uniformity.

2.4. High-performance liquid chromatography analysis of ibuprofen and ketoconazole

IBU and KETO were quantified by reversed-phase high-performance liquid chromatography (RP-HPLC) by Shimadzu HPLC Nexera series, equipped with a photodiode array detector and a SIL-40C autosampler, using the methods described in the literature [23,24], with some adjustments. The quantification of IBU was determined using Zorbax Eclipse Plus C18 column (150 mm × 4.6 mm, 5 μm particle size) with an isocratic elution mode. The mobile phase was acetonitrile, and water adjusted at pH 3.0 with HCl (0.1 M) in a ratio of volumes 60:40 (% v/v). The flow rate, injection volume, and column temperature were 2 mL/min, 20 μL, and 30 °C respectively. The spectrophotometric detector was operated at a wavelength of 230 nm. For KETO, Zorbax Eclipse Plus C18 column (150 mm × 4.6 mm, 5 μm particle size) was used as the stationary phase and the mobile phase was composed of methanol, and phosphate buffer 0.02 M at pH 8.0 in a ratio volume 80:20 (% v/v). The spectrophotometric detector was operated at a wavelength of 255 nm, the column temperature was set at 25 °C, the injection volume was 20 μL, and the flow rate at 1.0 mL/min.

2.5. Characterization of microbeads

2.5.1. Yield, encapsulation efficiency, and drug loading

The yield percentage (Y %) of the process was determined using Eq. (1)

$$Y\,\% = \frac{Mass\ microbeads}{Theorical\ mass\ of\ feed\ components} \times 100 \quad (1)$$

where mass microbeads is the amount of microbeads obtained after the lyophilization process and theoretical mass is the amount of drugs and polymers used to prepare the formulations.

The percentage of encapsulation efficiency (EE %) was computed using Eq. (2):

$$EE\,\% = \frac{Actual\ loading}{Theorical\ loading} \times 100 \quad (2)$$

where the actual loading is the drug content present in the sample and the theoretical loading is the theoretical amount of drug that should be present in the weighed microbeads. To determine IBU or KETO actual loading in the microbeads, an accurately weighed amount of each formulation (F_aIBU, F_bIBU, F_aKETO, and F_bKETO) was dissolved in 10 mL of methanol and water in a ratio of volumes 50:50 (v/v), and Ultraturrax T 25 basic was used to facilitate complete disaggregation of the microbeads. The solutions were filtered through a 0.22 μm membrane filter in polytetrafluorethylene (PTFE) and the concentration of the drugs was determined by the HPLC methods described above. Finally, drug loading (DL) was calculated as the real amount of drug (μg) in 100 mg of formulation.

The analyses were conducted in triplicate for each formulation and reported as the mean ± standard deviation (SD).

2.5.2. Microbeads size and morphology

The sizes of all microbeads were measured by optical microscopy (Inverted Laboratory Microscope Optech IB 4) equipped and interfaced with an image analysis program (Capture 2.1 software). For each formulation, at least fifty microbeads were examined to evaluate the mean diameter and their relative standard deviations. To assess the size homogeneity of microbeads in each production batch, the width of the particle distribution (Span), as defined in Eq. (4), was evaluated.

$$Span\ value = \frac{D_{90} - D_{10}}{D_{50}} \quad (4)$$

where D_{10}, D_{50}, and D_{90} represent the diameters of 10, 50, and 90 % of the sample particles, respectively [25].

The morphology of the microbeads was determined by scanning electron microscopy (SEM) using a Hitachi Tabletop Microscope TM300 and a secondary electron detector SED high vacuum mode, acceleration voltage 20 kV and EI Magnification 60 × –1000 × and interfaced with an analysis program (AZtecOne software). The microbeads or their section were sprinkled on an adhesive pad with electrical conductivity before being covered in a gold/palladium layer (sputter coating, 15–20 nm).

Furthermore, a chemical microanalysis test was conducted on the F_{6b}KETO formulation to assess the distribution of boron atoms associated at H_3BO_3 on the surface of the microbeads crosslinked with PVA.

2.6. Solid state characterization

Solid-state characterization of the drugs in all formulations was carried out using Fourier transform infrared spectroscopy (FT-IR), differential scanning calorimetry (DSC), and X-Ray Powder Diffraction (XRPD). FT-IR spectra were sampled in KBr pellets (2 % of the sample) and were analyzed with the PerkinElmer FT-IR Spectrophotometer 1600. Data were acquired between 4000 cm^{-1} and 400 cm^{-1}.

Thermal analyses by DSC were acquired using Mettler Toledo DSC1. The operative conditions for the DSC analysis were: sample weight 2–10 mg, scanning speed 5 °C/min, and range of temperature between 25 °C and 200 °C under 50 mL/min N_2 flow. The samples were heated in 40 μL aluminium pans with a hermetically closed lid. An empty pan was used as a reference.

The diffraction patterns were collected by using a Stoe StadiP 611 diffractometer.

Measurements were performed in transmission geometry with Cu-Kα1 radiation. Scans were carried out from 0 to 36° 2θ simultaneously (step width of 0.03° 2θ, 30 s/step).Samples have been prepared in a combinatorial 96-well plate (comprising an X-ray amorphous foil at the bottom).

2.7. Drug release study

Release studies were conducted on F_{6a}IBU, F_{6b}IBU, ASD-IBU, F_{6a}KETO, F_{6b}KETO, and ASD-KETO using the VanKel system VK 7000 with the rotational speed of the paddle set at 100 rpm and the temperature of the dissolution medium was maintained at 37 ± 0.5 °C. To generate sink condition, enough microbeads of each formulation were placed in 100 mL of medium to obtain a final IBU and KETO concentration of 50 μg/mL. In detail, IBU release was studied using a simulated gastric medium, SGF (0.1 M HCl, pH 1.2) for 2 h, while KETO release was analyzed in phosphate buffer, simulating enteric conditions, SIF (0.07 M PBS, pH 6.8) for 3 h. Samples with a volume of 1 mL were withdrawn at specific times and replaced with fresh medium to maintain constant volume. Samples were filtered (0.22 μm membrane filter in CA) and analyzed by RP-HPLC to determine the cumulative percentage of drug released.

2.8. Kinetics model drugs release

The data from the release studies of the F_{6a}IBU, F_{6b}IBU, ASD-IBU, F_{6a}KETO, F_{6b}KETO, and ASD-KETO formulations were evaluated using mathematical models, including a zero-order model (cumulative percentage of drug released vs. time), a first-order model (log cumulative percentage of drug remaining vs. time), the Higuchi model (cumulative percent drug released vs. square root of time), the Korsmeyer-Peppas model (log cumulative percent drug remaining vs. log time), and the Hixson-Crowell model (cubic root percent drug remaining vs. log time). These models were employed to interpret the kinetics of IBU and KETO release from microbeads and ASDs.

2.9. Stability study

The stability test was performed to assess the physical-chemical stability of all formulations (F_{6a}IBU, F_{6b}IBU, ASD-IBU, F_{6a}KETO, F_{6b}KETO, and ASD-KETO). Aliquots of each formulation were stored in a vial with and without a cap in a Climacell 222 – ECO line climatic chamber (MMM Group, Semmelweis Strasse, München, Germany) at 40 ± 0.5 °C and 75 % of RH for 4 weeks. Subsequently, DSC, FT-IR, and X-ray were conducted on each sample to evaluate solid-state stability, while an exact quantity of microbeads and ASDs was dissolved to quantify the drug and evaluate the chemical stability of IBU and KETO.

2.10. Statistical analysis

The experimental data are reported as the mean ± SD (standard deviation). Statistical analyses were conducted using Graph Prism version 8.0 (GraphPad Software Inc., La Jolla, CA, USA). Statistically significant differences were determined through Ordinary one-way ANOVA analysis of variance (ANOVA), followed by Bonferroni's post hoc tests. A probability level of **p < 0.0021 was considered significant (p value style: ****p < 0.0001, ***p < 0.0002,**p < 0.0021, p*<0.0332).

3. Results and discussions

3.1. Feed and consolidation bath selection

In literature, the use of PVA and SA to generate microbeads has been described by several groups using a syringe-dropping method [26,27]. However, in this work, PVA 3–82 was processed for the first time as a polymer feed in the prilling/vibration technique. The choice of the best polymer feed is a critical aspect of the prilling/vibration process as its properties directly affect processability and can have a significant impact on the characteristics of the final products [28]. In this technique, two important method variables are the processability of the polymeric feed and the consolidation of the microdroplets produced. Processability is understood as the ability of the solution to produce a laminar flow that can be broken up by applying a vibration force and the capacity to obtain well-consolidated and separated microbeads. Viscosity is certainly one of the most important variables in this technique; in fact, prilling can only able to process solutions with viscosity values of less than a few hundred mPa·s [29] and it is essential to study this parameter to predict the ability to flow laminarly through the nozzle. For this reason, preliminary studies on different types of PVA with different molecular weights were conducted and they are described in S1 of Supplementary Materials. Subsequently, the study was focused on PVA 3–82; the viscosity of PVA 3–82 solutions at 6, 9, and 20 % were 4.69, 9.61, and 87.32 mPa s, respectively. Thus, all solutions could be processed by prilling/vibration technology. Ultimately, the concentration of 20 % w/v was chosen as optimal for subsequent studies because the increase in the quantity of polymer led to the production of a more compact and handy microbead structure. Therefore, due to its low viscosity and high processability, the 20 % w/v solution of PVA 3–82 (S_0) was selected as the polymer feed.

Secondly, the selection of a consolidation bath plays a key role in the formation of microbeads. PVA is a difficult polymer to gel in an aqueous gelling bath, however, as it is documented in the literature, PVA can be cross-linked by various bifunctional and polyfunctional condensing agents, such as dianhydrides, glutaraldehyde, hexamethylene diisocyanate, and H_3BO_3 [30]. In this work, H_3BO_3 was used as the cross-linking agent because of its biocompatibility and non-toxicity [31]. It promoted PVA cross-linking through diol complexation, involving two diol units of two different chains of PVA and one borate ion through coordinative bonds [32,33]. Nevertheless, the consolidation of the S_0 feed in a gelling bath composed of solely 0.4 M H_3BO_3 did not produce microbeads but aggregates with low resistance. Therefore, other aqueous gelling baths were tested to obtain favorable conditions to produce microbeads e.g., $CaCl_2$ 0.3 M (a-bath) and $CaCl_2$ 0.18 M with added H_3BO_3 0.4 M (b-bath). For the use of these gelling baths, SA was added to the polymeric feed to produce rapid consolidation in the presence of biovalent ions (Ca^{++}) [34]. Furthermore, the addition of SA prevents the aggregation of PVA microbeads that occurs when they are cross-linked H_3BO_3 solely [31]. Different weight ratios of PVA and SA were tested S_1–S_6 (100:1, 71:1, 50:1, 33.:1, 25:1, 19:1) but the S_6 feed was the best performing due to the highest amount of SA, which allowed for greater cross-linking, resulting in the formation of microbeads that could be easily recovered from the consolidation bath. Therefore, feed S_6 was chosen for further studies and to investigate the influence of the consolation bath on the characteristics of the microbeads produced, two different baths (a and b) were adopted, resulting in F_{6a} and F_{6b}.

3.2. Production of placebo microbeads

The previous study provides us with information on the possibility of obtaining microbeads by prilling/vibration technique, but for our purposes, it is also essential to evaluate some critical quality attributes, such as yield, size, and size distribution of the microbeads. High yields minimize material consumption and reduce the economic expense of scaling up the process. The optimal size and the uniform size distribution ensure consistent dosing and prevent the risk of suffocation, particularly in infants and young children [35] or small animals.

As shown in Table 2, the F_{6a} formulation has a yield value of 45 % indicating that SA ensured the formation of microbeads, but most of the PVA was still lost in the consolidation bath. In contrast, F_{6b} has a 70 % higher yield due to the addition of H_3BO_3 in the consolidation bath used. In fact, the –OH groups of the PVA were cross-linked with H_3BO_3 to form a clathrate [27] that prevented leakage into the consolidation bath. H_3BO_3 greatly influenced the strength of the gel formed during consolidation, as initially, the gelling reaction is immediate on the surface of the microbeads and then allows further diffusion of the H_3BO_3 into the microbeads resulting in the polymerization of the PVA and formation of well-structured microbeads [36]. Therefore from the yield values, F_{6b} can be determined as a better solution than F_{6a}. Nevertheless, the yield value could be further improved by going to evaluate baths with additional bivalent agents, with different concentrations of gelling agents, or by going to further modulate the PVA/SA ratio.

F_{6a} generated microbeads with a diameter of about 1605 μm while F_{6b} produced microbeads with a diameter of 2050 μm (Table 2). The use of the b-bath produced larger microbeads than those obtained in a-bath, although the same nozzles were used, probably because of the greater consolidation of PVA by the H_3BO_3 that produced a better cross-linked and more compact structure. These sizes are in the range preferred for a pediatric or veterinary formulation because small particulates may be easier swallowed and thus more acceptable than single-unit formulations [37]. The diameters outlined in the FDA guidelines are accepted as appropriate for pediatric populations, including infants. In fact, to increase acceptability in pediatric age, a diameter of 2 mm should be used for children up to 6 months and 4 mm for those one-year-old [35].

SEM analysis (Fig. 1) of the F_{6b} microbeads showed an almost

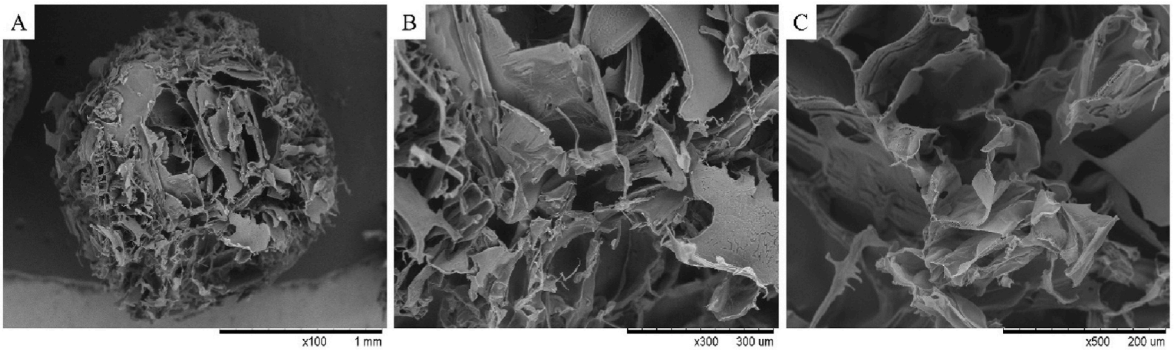

Fig. 1. SEM images of F_{6b} (A), enlargement of its surface (B and C).

spherical structure, a well-cross-linked structure with jagged edges. Fig. 1B and C shows an enlarger of the surface of the F_{6b} formulation showing a honeycomb structure with evenly distributed layers that allows the drug to be housed, and a very porous structure and numerous cavities are observed.

Most probably, sublimation during freeze-drying of the frozen water droplets resulted in the formation of irregular, porous structures, and a partial collapse of the polymer network [38].

In addition, a microanalysis was performed on the F_{6b} formulation (Fig. 2) to assess the distribution of boron atoms on the surface of the microbeads. Boron (blue in Fig. 2B and C) showed a homogeneous distribution on the particles.

3.3. Preparation and characterization of drug-loaded microbeads

This placebo-based preliminary study allowed us to identify the parameters for the production of microbeads that were loaded with IBU or KETO. The quantity of loaded drugs (0.15 % w/v) was higher than the calculated solubility drugs in the S_6 polymeric feed. The presence of PVA improved the solubility compared to water, by increasing it 5-fold for IBU (0.108 mg/mL) and 36-fold for KETO (0.277 mg/mL), as detailed in S2 of the Supplementary Material. Despite the resulting feed being a suspension, it remained easily processable. Like the placebo, S_6IBU and S_6KETO feeds were consolidated in a-bath to obtain F_{6a}IBU and F_{6a}KETO formulations or b-bath to produce F_{6b}IBU and F_{6b}KETO formulations. The EE %, drug loading, and production yield of the microbeads are shown in Table 3. Notably, the yield of the F_{6b}IBU and F_{6b}KETO formulations is higher than that of F_{6a}IBU and F_{6a}KETO due to the presence of H_3BO_3 in the consolidation bath. The encapsulation efficiency of the F_{6a}IBU formulation is lower than the F_{6a}KETO formulation because IBU tends to diffuse into the consolidation bath due to the higher water solubility of IBU compared to KETO [20,39]. However, in the F_{6b}IBU formulation, the efficiency is considerably higher than in F_{6a}IBU. This is because the cross-linking of PVA with H_3BO_3 creates a structure that traps the drug more effectively, reducing diffusion into the consolidation bath. Similarly, the F_{6b}KETO formulation shows increased efficiency compared to the F_{6a}KETO due to the enhanced structure of the microbeads. DL values for F_{6a}IBU and F_{6a}KETO ranged from 500.34 to 1117.21 μg of drug per 100 mg of beads, while for F_{6b}IBU and F_{6b}KETO, they varied from 560.06 to 735.72 μg of drug per 100 mg of microbeads. Furthermore, increasing the amount of drug by 4 or 14-fold improved the EE values (Table S3 in Supplementary Materials), indicating that the percentage of drug-loaded did not affect production. This highlights that the proposed method is highly versatile and allows microbeads with different drug loadings to be obtained, meeting different therapeutic needs.

Table 3
Yield %, EE %, DL, and size of the dried microbeads. Data are reported as the mean ± SD.

Formulation Code	Yield %	EE %	DL*	Diameter microbeads (μm)
F_{6a}IBU	42.45 ± 5.43	32.92 ± 3.88	500.34 ± 21.33	1581 ± 272
F_{6a}KETO	45.08 ± 8.13	52.77 ± 8.43	1117.21 ± 30.48	1676 ± 217
F_{6b}IBU	68.88 ± 2.62	67.04 ± 3.15	560.06 ± 10.25	2027 ± 204
F_{6b}KETO	65.16 ± 5.58	63.65 ± 4.89	735.72 ± 22.37	2125 ± 208

DL* is expressed as μg of drug in 100 mg of microbeads.

The mean diameters of the microbeads after lyophilization are listed in Table 3. The diameters were less than 1676 μm for F_{6a}IBU and F_{6a}KETO and less than 2125 μm for F_{6b}IBU and F_{6b}KETO. Similar to placebo formulations, the size of these microbeads varies considerably depending on the consolidation bath used. Finally, the size distribution was assessed by estimating the span value, as shown in Table 4. A span value of 0 indicated a monodisperse particle size distribution. Therefore, all span values obtained confirm a strictly monodisperse size distribution.

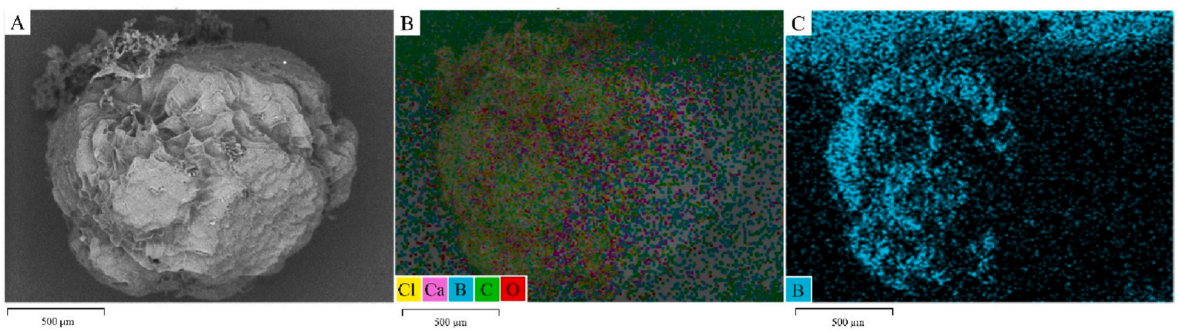

Fig. 2. Microanalysis images of F_{6b} surface.

Table 4
Diameter D50, D10, and D90 and SPAN of microbeads.

Formulation Code	D_{50}	D_{10}	D_{90}	Span
F_{6a}IBU	1581 ± 272	1453 ± 58	1735 ± 219	0.18
F_{6a}KETO	1676 ± 217	1525 ± 103	1865 ± 173	0.20
F_{6b}IBU	2027 ± 204	1869 ± 37	2186 ± 110	0.16
F_{6b}KETO	2125 ± 208	1973 ± 98	2269 ± 123	0.14

3.4. Preparation and characterization of ASDs

ASDs are a useful and very common method for improving the solubility and the dissolution rate of poorly water-soluble drugs. ASDs can be manufactured by several methods. The solvent evaporation technique is a widely used method in the laboratory that depends mainly on the common solvation potential of excipients and drug and solvent evaporation [40]. In fact, this method involved the use of a volatile solvent which is easily removed due to its low boiling point. Despite being a simple method, the most challenging aspect is to obtain a solvent system capable of solubilizing the drug-polymer system and not being toxic, as toxicity occurs due to the difficulty of removing the residual solvent from the formulation [41]. Aqueous solvents can also be used in combination with organic solvents to increase the solubility of the polymer and/or reduce their use [42], but in this case, an increase in boiling temperature may occur, which could lead to degradation of the drug. Furthermore, a drawback of ASD was their poor scale-up for the purposes of manufacturing [43]. In this work, a mixture of ethanol-water at a volume ratio of 50:50 (% v/v) was used to produce ASDs. This choice was made because PVA is insoluble in organic solvents, necessitating a high-water fraction. Additionally, at the same time, a high quantity of organic solvent is needed to allow rapid evaporation at temperatures lower than the boiling point of water. For ASDs produced (ASD-IBU and ASD-KETO), a vitreous powder was collected that was difficult to remove from the flask and was subsequently sieved to ensure a uniform dimension. ASD-IBU and ASD-KETO were characterized for yield, EE, and DL (Table 5). The EE is very high but the difficulty in recovering the powder and the subsequent sieving process resulted in very low production yields of 13 % lower than the prilling/vibration technique that could be considered for industrial scale-out production [29].

3.5. Characterization of the solid-state on microbeads and ASDs

Solid-state characterization was carried out by FT-IR, DSC, and XRPD to assess whether F_{6a}IBU, F_{6b}IBU, F_{6a}KETO, and F_{6b}KETO produced using prilling/vibration technique induced amorphization of the drug comparable to that obtained from ASD-IBU and ASD-KETO.

IBU and KETO have a strong endothermic peak about at 77–78 °C and 152 °C, respectively, due to the melting of their crystalline state [44,45]. In contrast, the thermograms in Fig. 3 show that in both ASDs (ASD-IBU and ASD-KETO) and microbeads (F_{6b}IBU and F_{6b}KETO), the endothermic peak of IBU and KETO is completely absent, indicating that in both cases the amorphization process of the drug was induced during the production and/or lyophilization phase. However, in both the F_{6a}IBU and F_{6a}KETO formulations at 75 °C, there is a large endothermic peak due to water, which doesn't allow the evaluation of the eventual endothermic peak of the drug, which probably as in the other formulations is present in amorphous form.

Fig. 4A shows the diffraction patterns of IBU, ASD-IBU, F_{6a}IBU, and F_{6b}IBU while Fig. 4B describes the diffraction patterns of KETO, ASD-KETO, F_{6a}KETO, and F_{6b}KETO. The sharper peaks present in the diffraction pattern of IBU and KETO indicate its crystallinity, while their complete disappearance in the formulations clearly shows the amorphization of the drugs as already determined by DSC results. The results of the DSC and XRPD are further supported by FT-IR data, discussed in the S5 of Supplementary Materials.

Table 5
Yield %, EE %, and DL of ASDs. Data are reported as the mean ± SD.

Formulation Code	Yield %	EE %	DL*
F_{6a}IBU	12.79 ± 3.61	96.03 ± 0.83	711.62 ± 3.64
F_{6a}KETO	13.89 ± 2.78	97.07 ± 0.07	727.25 ± 7.69

DL* is expressed as μg of drug in 100 mg of powder.

3.6. Drug release study of microbeads and ASDs

Release studies were performed to evaluate how the characteristics of studied formulations were able to influence the drug release. Indeed, for weakly acidic and basic drugs such as IBU and KETO, their solubility and systemic absorption depend on the pH of the local gastrointestinal environment. In general, oral absorption of weakly acidic drugs may be less problematic due to a longer residence time in the small intestine with favorable pH conditions facilitating dissolution and absorption; however, gastric emptying may still be important in determining the oral absorption of drugs. On the other hand, weakly basic drugs have the potential to supersaturate and precipitate when the drug passes from the stomach, a favorable pH environment, to the proximal small intestine, an unfavorable pH environment [46]. Since microbeads predominantly contain PVA, they dissolve in a pH-independent manner, showing the same solubilization performance throughout the gastrointestinal tract [47], which could result in a better dissolution of IBU in the gastric environment and KETO in the intestinal environment. In the last case, the microbeads could be placed in a gastroresistant capsule or coated with a gastroresistant polymer to avoid rapid solubilization of KETO (given its high solubility value) and repecipitation in the intestinal tract. Furthermore, the release profile of ASD-IBU and ASD-KETO was analyzed to compare them to the dissolution profiles of the microbeads.

The release profiles of IBU, ASD-IBU, F_{6a}IBU, and F_{6b}IBU in SGF at pH 1.2 are shown in Fig. 5A. The cumulative percentage of IBU released in SGF after 2 h was 90 %, 96 %, and 79 % from ASD-IBU, F_{6b}IBU, and F_{6a}IBU respectively; with a 2.5-fold increase in ASD-IBU and F_{6b}IBU over the drug alone (42 %). The F_{6b}IBU microbeads initially showed a similar profile to the F_{6a}IBU microbeads, in fact in the first few minutes they showed a rapid release of the drug into the dissolution medium, probably the drug most available to be released, i.e. the one located in the most superficial part of the microbeads. Subsequently, at 60 min the F_{6a}IBU microbeads showed a lower release than the F_{6b}IBU ($p < 0.0021$) formulation this could be because SA tended to form an alginic acid gel at acidic pH that was insoluble and retarded the release of the drug; however, in the F_{6b}IBU formulation, SA was less cross-linked as the degree of cross-linking increases with the $CaCl_2$ concentration [48], so the drug is released faster. The release profile of ASD-IBU was superimposable on both F_{6a}IBU and F_{6b}IBU formulation, however, after 2 h in SGF the cumulative percentage of IBU release from ASD-IBU was 90 % like that obtained for F_{6b}IBU (96 %).

The release profiles of KETO, ASD-KETO, F_{6a}KETO, and F_{6b}KETO in SIF at pH 6.8 are shown in Fig. 5B. As can be seen from Fig. 5B, KETO showed low dissolution at pH 6.8 due to its low solubility. The release values of the different formulations (F_{6a}KETO, F_{6b}KETO, and ASD-KETO) showed a significant difference ($p < 0.0001$) after 3 h compared to the dissolution value of the drug alone. Approximately 86 % of the drug was released from both F_{6a}KETO and F_{6b}KETO, showing a 36-fold increase in the rate of KETO dissolution from the microbeads compared to the drug alone (2 %). For the F_{6a}KETO formulation, a burst release effect was observed in the first 15 min, probably because the release of KETO from the microbeads was controlled by the degree of cross-linking of the SA by calcium. Calcium alginate, in contact with intestinal fluids (pH 6.8) can hydrate and swell, allowing the diffusion of the drug and its rapid dissolution [49]. In contrast, the F_{6b}KETO formulation showed at 15 min a significantly ($p < 0.0001$) different release than F_{6a}KETO. This different release of the drug from the microbeads was associated with the greater cross-linking due to both the

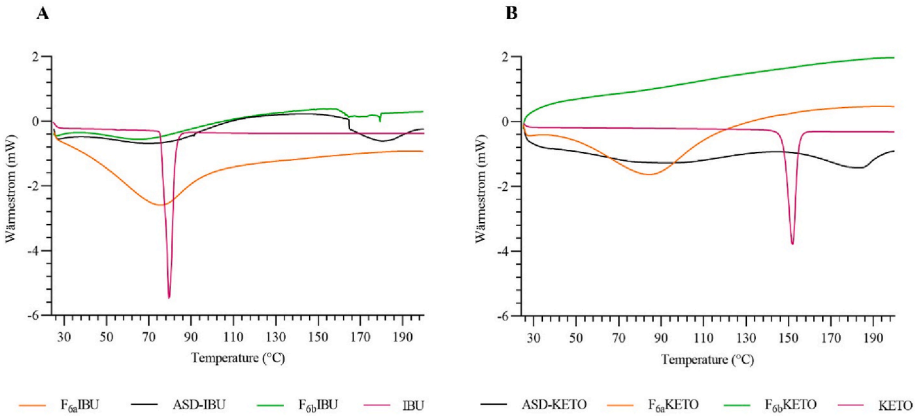

Fig. 3. (A) Thermograms of formulations ASD-IBU, F_{6a}IBU, and F_{6b}IBU; (B) Thermograms of formulations ASD-KETO, F_{6a}KETO, and F_{6b}KETO.

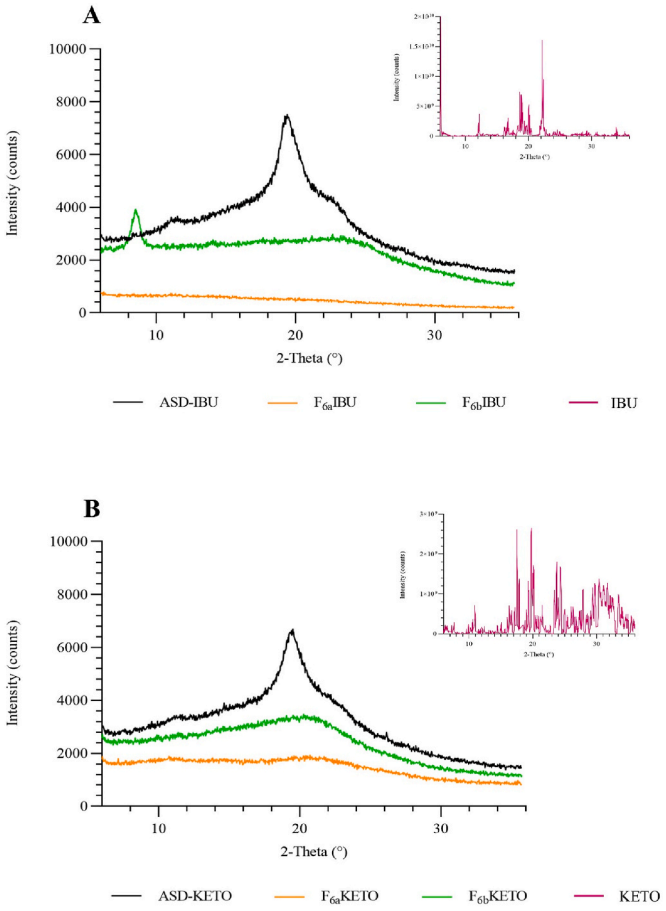

Fig. 4. (A) Diffractograms of formulations ASD-IBU, F_{6a}IBU, and F_{6b}IBU; (B) Diffractograms of formulations ASD-KETO, F_{6a}KETO, and F_{6b}KETO.

presence of the SA but also the PVA, which produced a denser network that hinders dissolution and degradation of the microbeads resulting in a more controlled release of the drug. The degree of cross-linking was strictly correlated with the swelling properties [50,51] and the results indicated that the high cross-linking density of the microbeads obtained with H_3BO_3 resulted in the absorption of less water with a consequent reduction of the channels from which the drug a more gradual release of KETO. The release profile of ASD-KETO overlapped with that of F_{6b}KETO showing a drug release of 90 % after 3 h in SIF.

The produced microbeads showed the same release profile as ASDs but, microbeads can be a promising alternative as they do not require an organic solvent for preparation and could allow industrial scale-out production.

3.7. Kinetic model

Kinetic models provide information on drug release behavior from a formulation, which depends on several factors, including the type of polymer matrix encapsulating the drug, the degree of cross-linking, and the pH of the release study environment [52]. Release data were fitted to the most common kinetic models, as shown in Table 6, to understand the mechanism of IBU or KETO release from microbeads and ASDs, except for F_{6a}KETO, which exhibited a complete release by burst effect within the first 15 min. Regardless of drug type and dissolution medium, ASD-IBU and ASD-KETO show diffusive kinetics confirmed by Higuchi-Connors linear regression coefficients (R^2) 0.993 and 0.947, respectively. Higuchi's model describes drug release as a diffusion process, in which drug molecules move from regions of high concentration (within ASDs) to regions of low concentration (surrounding medium). This model is particularly applicable to matrix-type systems, in which the drug is uniformly dispersed within a polymer matrix. Additionally, the Korsmeyer-Peppas equation is also applicable; in fact, values of n less than 0.4 and R^2 (0.993 and 0.968) indicate that drug release from ASDs fits a Fickian-diffusive release mechanism [53,54]. Among all the models studied, the Korsmeyer-Peppas model for F_{6a}IBU was found to best describe the release profile of the formulation (R^2 = 0.978). The Korsmeyer-Peppas model is used when the release mechanism is complex and may involve more than one type of release phenomenon, such as diffusion, erosion, or swelling [55]. The value of n less than 0.2 suggests that the rate of drug release is not simply controlled by Fickian diffusion but may involve more complex interactions within the polymer matrix, such as the presence of SA in the polymer matrix, which conditions drug release in acidic environments. The release kinetics of F_{6b}KETO fit according to first-order kinetics (R^2 = 0.952), likely influenced most by PVA cross-linking with H_3BO_3, making the release profile proportional to the amount of drug in the formulation. Differently, F_{6b}KETO fits better with Higuchi-Connors kinetics (R^2 = 0.925), supporting the idea that drug release is more influenced by diffusion processes due to the presence of SA in the polymer matrix, which dissolves and swells at pH 6.8, than by PVA cross-linking.

3.8. Stability study

The formulations (F_{6a}IBU, F_{6b}IBU, ASD-IBU, F_{6a}KETO, F_{6b}KETO, and ASD-KETO) underwent accelerated stability studies at 40 °C/75 % RH for 4 weeks. They were stored in vials, with some vials being capped and others uncapped. The aim was to assess chemical degradation and physical changes. The solid-state's physical stability was evaluated using DSC, XRPD, and FT-IR, while chemical stability was assessed

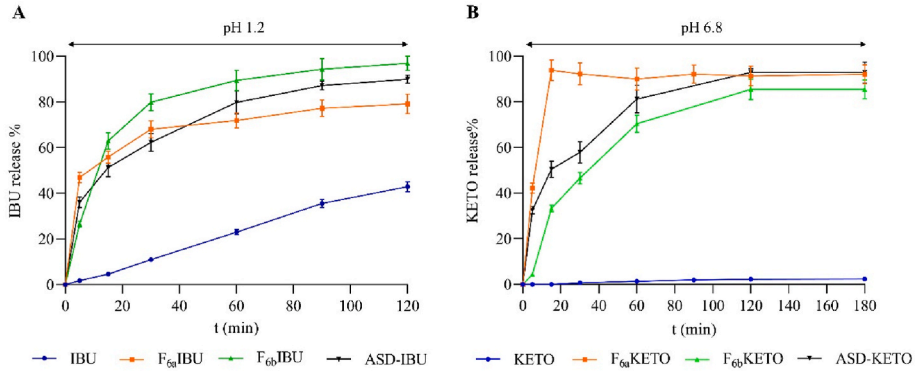

Fig. 5. (A) Drug release profile of IBU, ASD-IBU, F_{6a}IBU, and F_{6b}IBU in simulated gastric fluids at pH 1.2; (B) Drug release profile of KETO, ASD-KETO, F_{6a}KETO, and F_{6b}KETO simulated enteric fluid at pH 6.8.

Table 6
Mathematical models of IBU and KETO release kinetics from ASD-IB, F_{6a}IBU, F_{6b}IBU, ASD-KETO, F_{6a}KETO, and F_{6b}KETO formulations.

Formulation Code	Zero order model		First order model		Higuchi-Connors model		Korsmeyer-Peppas model		Hixson Crowell model	
	k	R^2	k	R^2	k	R^2	n	R^2	k	R^2
ASD-IBU	36.364	0.742	−0.470	0.949	60.981	0.933	0.296	0.993	−1.229	0.895
F_{6a}IBU	26.762	0.546	−0.271	0.753	48.019	0.786	0.168	0.978	−0.714	0.685
F_{6b}IBU	39.819	0.663	−0.717	0.952	68.557	0.878	0.383	0.868	−1.466	0.866
ASD-KETO	25.060	0.682	−0.386	0.893	52.599	0.898	0.304	0.968	−0.857	0.841
F_{6b}KETO	27.703	0.761	−0.299	0.892	55.875	0.925	0.772	0.834	−0.764	0.857

through drug loading estimation.

Evaluation of drug loading was performed at t_0 and t_4 using the conditions above indicated the data are reported in Table 7. The data showed that the concentration of IBU and KETO in the ASDs after 4 weeks in vials with a cap remained constant. However, a decrease in drug concentration was observed in all formulations stored in vials without caps, indicating that exposure to conditions such us direct contact with moisture could lead to potential drug degradation. For the F_{6a}IBU formulation in a vial with a cap, about 23.84 % of IBU was observed after 4 weeks. In contrast, for the F_{6b}IBU formulation in a vial with a cap, the residual IBU was 91.12 % with a 9 % reduction in the amount of drug, indicating that the F_{6b}IBU formulation compared to F_{6a}IBU is significantly more stable due to the higher cross-linking power, which allows the formation of a structure that better protects the loaded drug.

The DSC and XRPD results demonstrated the absence of any change in the thermograms and diffractograms, respectively, during the stability period of all formulations (Figs. S4 and S5 in Supplementary Materials). This indicates that the amorphous state of the drugs was successfully maintained in all formulations without any crystallization/polymorphic transformation events. However, a broad dehydration peak for $F_{6a}IBU_{open}$ at around 90 °C that extended to around 110 °C was observed in the DSC thermogram, due to the absorption of moisture under high humidity conditions during the period of stability due to the absence of the stopper in the storage vials. A similar peak was observed in the $F_{6a}KETO_{open}$ formulation between 120 and 150 °C probably due to the high moisture content.

Table 7
Drug % in the formulations at t_0, t_4 weeks at 40 ± 0.5 °C and 75 %. Data are reported as the mean of results ± SD.

Formulation Code	Drug % (t_0)	Drug % ($t_{4\ in\ vials\ closed}$)	Drug % ($t_{4\ in\ vials\ open}$)
ASD-IBU	100	99.98 ± 0.52	91.12 ± 0.98
ASD-KETO	100	99.97 ± 0.10	85.59 ± 0.72
F_{6a}IBU	100	23.84 ± 2.85	16.77 ± 1.83
F_{6b}IBU	100	91.12 ± 5.41	85.90 ± 6.85
F_{6a}KETO	100	99.92 ± 1.89	62.14 ± 4.26
F_{6b}KETO	100	99.76 ± 0.67	96.35 ± 2.87

4. Conclusions

This work focused on producing IBU or KETO-loaded PVA/SA microbeads using the prilling/vibration technique to enhance drug solubility and dissolution rate. The study also looked at finding the most suitable consolidation baths. Combining $CaCl_2$ and H_3BO_3 in the consolidation bath resulted in more compact and durable microbeads with high yield and encapsulation efficiency. The microbeads produced were fully characterized and compared to another technological approach, such as ASDs, to evaluate if they show similar improvements in solubility and dissolution rate. In conclusion, all formulations met the proposed objectives. Additionally, the microbeads offered a high level of dosing flexibility, making them suitable for administration in pediatric or veterinary patients with swallowing difficulties and requiring customized dosing.

CRediT authorship contribution statement

Marianna Ivone: Writing – original draft, Methodology, Investigation. **Nunzio Denora:** Writing – review & editing, Supervision, Conceptualization. **Vita D'Amico:** Methodology, Data curation. **Lena Mareczek:** Writing – review & editing, Formal analysis, Data curation. **Lena Karin Mueller:** Writing – review & editing, Validation, Formal analysis, Data curation. **Ilaria Arduino:** Data curation. **Alessandra Ambruosi:** Writing – review & editing, Supervision. **Angela Assunta Lopedota:** Writing – review & editing, Supervision, Methodology, Conceptualization.

Declaration of competing interest

The authors declare that they have no known competing financial interests or personal relationships that could have appeared to influence the work reported in this paper.

Data availability

Data will be made available on request.

Acknowledgments

We thank Bernd Kuestner's team for the XRPD and DSC measurements; Corina-Madalina Birgau and Laura Halstenberg for the viscosity measurements, DSC and XRPD data; Mr. Pasquale Trotti (DISSPA UNIBA) for his contribution to SEM analysis and microanalysis.

Appendix A. Supplementary data

Supplementary data to this article can be found online at https://doi.org/10.1016/j.jddst.2024.105974.

References

[1] A.A. Oun, G.H. Shin, J.-W. Rhim, J.T. Kim, Recent advances in polyvinyl alcohol-based composite films and their applications in food packaging, Food Packag. Shelf Life 34 (Dec. 2022) 100991, https://doi.org/10.1016/j.fpsl.2022.100991.
[2] L.K. Mueller, L. Halstenberg, N. Di Gallo, T. Kipping, Evaluation of a Three-fluid nozzle spraying process for facilitating spray drying of hydrophilic polymers for the creation of amorphous solid dispersions, Pharmaceutics 15 (11) (Oct. 2023) 2542, https://doi.org/10.3390/pharmaceutics15112542.
[3] C.C. DeMerlis, D.R. Schoneker, Review of the oral toxicity of polyvinyl alcohol (PVA), Food Chem. Toxicol. 41 (3) (Mar. 2003) 319–326, https://doi.org/10.1016/S0278-6915(02)00258-2.
[4] M.-J. Choi, M.R. Woo, H.-G. Choi, S.G. Jin, Effects of polymers on the drug solubility and dissolution Enhancement of poorly water-soluble Rivaroxaban, Int. J. Mol. Sci. 23 (16) (Aug. 2022) 9491, https://doi.org/10.3390/ijms23169491.
[5] Srinath Muppalaneni, Polyvinyl alcohol in medicine and pharmacy: a perspective, J Dev Drugs 2 (3) (2013), https://doi.org/10.4172/2329-6631.1000112.
[6] D. Harris, E. Hermans, S. Klein, L. Wagner-Hattler, J. Walsh, Age-appropriate solid oral formulations for pediatric applications with a focus on multiparticulates and minitablets: summary of September 2019 EuPFI workshop, Eur. J. Pharm. Biopharm. 153 (Aug. 2020) 222–225, https://doi.org/10.1016/j.ejpb.2020.06.012.
[7] J. Breitkreutz, J. Boos, Paediatric and geriatric drug delivery, Expet Opin. Drug Deliv. 4 (1) (Jan. 2007) 37–45, https://doi.org/10.1517/17425247.4.1.37.
[8] F.L. Lopez, T.B. Ernest, C. Tuleu, M.O. Gul, Formulation approaches to pediatric oral drug delivery: benefits and limitations of current platforms, Expet Opin. Drug Deliv. 12 (11) (Nov. 2015) 1727–1740, https://doi.org/10.1517/17425247.2015.1060218.
[9] D. Khan, D. Kirby, S. Bryson, M. Shah, A. Rahman Mohammed, Paediatric specific dosage forms: patient and formulation considerations, Int. J. Pharm. 616 (Mar. 2022) 121501, https://doi.org/10.1016/j.ijpharm.2022.121501.
[10] C.F. da Silva, et al., New trends in drug delivery systems for veterinary applications, Pharm. Nanotechnol. 9 (1) (Mar. 2021) 15–25, https://doi.org/10.2174/2211738508666200613214548.
[11] E. Janus, et al., Enhancement of ibuprofen solubility and skin permeation by conjugation with <scp>l</scp> -valine alkyl esters, RSC Adv. 10 (13) (2020) 7570–7584, https://doi.org/10.1039/D0RA00100G.
[12] H.S. Ghazal, A.M. Dyas, J.L. Ford, G.A. Hutcheon, The impact of food components on the intrinsic dissolution rate of ketoconazole, Drug Dev. Ind. Pharm. 41 (10) (Oct. 2015) 1647–1654, https://doi.org/10.3109/03639045.2014.983114.
[13] Y. Moghadamnia, S. Kazemi, B. Rezaee, M. Rafati-Rahimzadeh, S. Ebrahimpour, F. Aghapour, New formulation of ibuprofen on absorption-rate: a comparative bioavailability study in healthy volunteers, Caspian J Intern Med 10 (2) (2019) 150–155, https://doi.org/10.22088/cjim.10.2.150.
[14] A.J. Garner, R. Saatchi, O. Ward, D.P. Hawley, Juvenile idiopathic arthritis: a review of novel diagnostic and monitoring technologies, Healthcare 9 (12) (Dec. 2021) 1683, https://doi.org/10.3390/healthcare9121683.
[15] E.H. Giannini, et al., Ibuprofen suspension in the treatment of juvenile rheumatoid arthritis, J. Pediatr. 117 (4) (Oct. 1990) 645–652, https://doi.org/10.1016/S0022-3476(05)80708-5.
[16] M.G. Papich, Ketoconazole, in: Papich Handbook of Veterinary Drugs, Elsevier, 2021, pp. 496–498, https://doi.org/10.1016/B978-0-323-70957-6.00288-0.
[17] A. Lopedota, et al., Spray dried chitosan microparticles for intravesical delivery of celecoxib: preparation and characterization, Pharm. Res. (N. Y.) 33 (9) (Sep. 2016) 2195–2208, https://doi.org/10.1007/s11095-016-1956-7.
[18] G.F. Racaniello, et al., Innovative pharmaceutical techniques for paediatric dosage forms: a systematic review on 3D printing, prilling/vibration and microfluidic platform, J. Pharmacol. Sci. (Tokyo, Jpn.) (Apr. 2024), https://doi.org/10.1016/j.xphs.2024.04.001.
[19] A.A. Lopedota, et al., From oil to microparticulate by prilling technique: production of polynucleate alginate beads loading Serenoa Repens oil as intestinal delivery systems, Int. J. Pharm. 599 (Apr. 2021) 120412, https://doi.org/10.1016/j.ijpharm.2021.120412.
[20] V. D'Amico, et al., Colonic budesonide delivery by multistimuli alginate/Eudragit® FS 30D/inulin-based microspheres as a paediatric formulation, Carbohydr. Polym. 302 (Feb. 2023) 120422, https://doi.org/10.1016/j.carbpol.2022.120422.
[21] V. D'Amico, et al., Investigating the prilling/vibration technique to produce gastric-directed drug delivery systems for misoprostol, Int. J. Pharm. 651 (Feb. 2024) 123762, https://doi.org/10.1016/j.ijpharm.2023.123762.
[22] M. Beneš, et al., Methods for the preparation of amorphous solid dispersions – a comparative study, J. Drug Deliv. Sci. Technol. 38 (Apr. 2017) 125–134, https://doi.org/10.1016/j.jddst.2017.02.005.
[23] O. Popovska, Z. Kavrakovski, V. Rafajlovska, A RP-HPLC method for the determination of ketoconazole in pharmaceutical dosage forms, Curr. Pharmaceut. Anal. 13 (6) (Sep. 2017), https://doi.org/10.2174/1573412912666160610104703.
[24] A. Spennacchio, A. Lopedota, F. la Forgia, S. Fontana, M. Franco, N. Denora, Physicochemical stability of the extemporaneous ibuprofen oral suspension in 'wagner' base, Int. J. Pharm. Compd. 27 (1) (2023) 72–77.
[25] R. Varela-Fernández, et al., Design, optimization, and in vitro characterization of idebenone-loaded PLGA microspheres for LHON treatment, Int. J. Pharm. 616 (Mar. 2022) 121504, https://doi.org/10.1016/j.ijpharm.2022.121504.
[26] S. Hua, H. Ma, X. Li, H. Yang, A. Wang, pH-sensitive sodium alginate/poly(vinyl alcohol) hydrogel beads prepared by combined Ca2+ crosslinking and freeze-thawing cycles for controlled release of diclofenac sodium, Int. J. Biol. Macromol. 46 (5) (Jun. 2010) 517–523, https://doi.org/10.1016/j.ijbiomac.2010.03.004.
[27] S. Wang, Q. Ma, R. Wang, Q. Zhu, L. Yang, Z. Zhang, Preparation of sodium alginate-poly (vinyl alcohol) blend beads for base-triggered release of dinotefuran in Spodoptera litera midgut, Ecotoxicol. Environ. Saf. 202 (Oct. 2020) 110935, https://doi.org/10.1016/j.ecoenv.2020.110935.
[28] G. Auriemma, P. Russo, P. Del Gaudio, C.A. García-González, M. Landín, R. P. Aquino, Technologies and formulation design of polysaccharide-based hydrogels for drug delivery, Molecules 25 (14) (Jul. 2020) 3156, https://doi.org/10.3390/molecules25143156.
[29] M. Whelehan, I.W. Marison, Microencapsulation using vibrating technology, J. Microencapsul. 28 (8) (Dec. 2011) 669–688, https://doi.org/10.3109/02652048.2011.586068.
[30] M.A. Teixeira, J.C. Antunes, M.T.P. Amorim, H.P. Felgueiras, Optimization of the crosslinking process with glutaraldehyde vapor in PVA based electrospun membranes to wound dressings applications, in: Proceedings of 2nd International Online-Conference on Nanomaterials, MDPI, Basel, Switzerland, Nov. 2020, p. 7906, https://doi.org/10.3390/IOCN2020-07906.
[31] M.A.P. Nunes, P.M.P. Gois, M.E. Rosa, S. Martins, P.C.B. Fernandes, M.H.L. Ribeiro, Boronic acids as efficient cross linkers for PVA: synthesis and application of tunable hollow microspheres in biocatalysis, Tetrahedron 72 (46) (Nov. 2016) 7293–7305, https://doi.org/10.1016/j.tet.2016.02.017.
[32] I. Yu Prosanov, S.T. Abdulrahman, S. Thomas, N.V. Bulina, K.B. Gerasimov, Complex of polyvinyl alcohol with boric acid: structure and use, Mater. Today Commun. 14 (Mar. 2018) 77–81, https://doi.org/10.1016/j.mtcomm.2017.12.012.
[33] R.V. Gadhave, S.K. V, P.V. Dhawale, P.T. Gadekar, Effect of boric acid on poly vinyl alcohol- tannin blend and its application as water-based wood adhesive, Des. Monomers Polym. 23 (1) (Jan. 2020) 188–196, https://doi.org/10.1080/15685551.2020.1826124.
[34] C.H. Goh, P.W.S. Heng, L.W. Chan, Alginates as a useful natural polymer for microencapsulation and therapeutic applications, Carbohydr. Polym. 88 (1) (Mar. 2012) 1–12, https://doi.org/10.1016/j.carbpol.2011.11.012.
[35] M. Trofimiuk, K. Wasilewska, K. Winnicka, How to modify drug release in paediatric dosage forms? Novel technologies and modern approaches with regard to children's population, Int. J. Mol. Sci. 20 (13) (Jun. 2019) 3200, https://doi.org/10.3390/ijms20133200.
[36] M.A.P. Nunes, H. Vila-Real, P.C.B. Fernandes, M.H.L. Ribeiro, Immobilization of naringinase in PVA–alginate matrix using an innovative technique, Appl. Biochem. Biotechnol. 160 (7) (Apr. 2010) 2129–2147, https://doi.org/10.1007/s12010-009-8733-6.
[37] A. Lopalco, et al., Taste masking of propranolol hydrochloride by microbeads of EUDRAGIT® E PO obtained with prilling technique for paediatric oral administration, Int. J. Pharm. 574 (Jan. 2020) 118922, https://doi.org/10.1016/j.ijpharm.2019.118922.
[38] T. Hu, Q. Liu, T. Gao, K. Dong, G. Wei, J. Yao, Facile preparation of tannic acid–poly(vinyl alcohol)/sodium alginate hydrogel beads for methylene blue removal from simulated solution, ACS Omega 3 (7) (Jul. 2018) 7523–7531, https://doi.org/10.1021/acsomega.8b00577.
[39] N.V.N. Jyothi, P.M. Prasanna, S.N. Sakarkar, K.S. Prabha, P.S. Ramaiah, G. Y. Srawan, Microencapsulation techniques, factors influencing encapsulation efficiency, J. Microencapsul. 27 (3) (May 2010) 187–197, https://doi.org/10.3109/02652040903131301.
[40] R.B. Chavan, A. Lodagekar, B. Yadav, N.R. Shastri, Amorphous solid dispersion of nisoldipine by solvent evaporation technique: preparation, characterization, in vitro, in vivo evaluation, and scale up feasibility study, Drug Deliv Transl Res 10 (4) (Aug. 2020) 903–918, https://doi.org/10.1007/s13346-020-00775-8.
[41] V.K. Nikam, S.K. Shete, J.P. Khapare, Most promising solid dispersion technique of oral dispersible tablet, Beni Suef Univ J Basic Appl Sci 9 (1) (Dec. 2020) 62, https://doi.org/10.1186/s43088-020-00086-4.
[42] S.V. Bhujbal, et al., Pharmaceutical amorphous solid dispersion: a review of manufacturing strategies, Acta Pharm. Sin. B 11 (8) (Aug. 2021) 2505–2536, https://doi.org/10.1016/j.apsb.2021.05.014.

[43] T. Vasconcelos, B. Sarmento, P. Costa, Solid dispersions as strategy to improve oral bioavailability of poor water soluble drugs, Drug Discov. Today 12 (23–24) (Dec. 2007) 1068–1075, https://doi.org/10.1016/j.drudis.2007.09.005.
[44] G. Bannach, et al., Thermoanalytical study of some anti-inflammatory analgesic agents, J. Therm. Anal. Calorim. 102 (1) (Oct. 2010) 163–170, https://doi.org/10.1007/s10973-010-0939-x.
[45] B. Karolewicz, A. Górniak, A. Owczarek, E. Żurawska-Płaksej, A. Piwowar, J. Pluta, Thermal, spectroscopic, and dissolution studies of ketoconazole–Pluronic F127 system, J. Therm. Anal. Calorim. 115 (3) (Mar. 2014) 2487–2493, https://doi.org/10.1007/s10973-014-3661-2.
[46] Y. Tsume, et al., The impact of supersaturation level for oral absorption of BCS class IIb drugs, dipyridamole and ketoconazole, using in vivo predictive dissolution system: gastrointestinal Simulator (GIS), Eur. J. Pharmaceut. Sci. 102 (May 2017) 126–139, https://doi.org/10.1016/j.ejps.2017.02.042.
[47] Y. Umemoto, et al., An effective polyvinyl alcohol for the solubilization of poorly water-soluble drugs in solid dispersion formulations, J. Drug Deliv. Sci. Technol. 55 (Feb. 2020) 101401, https://doi.org/10.1016/j.jddst.2019.101401.
[48] J. Li, Y. Wu, J. He, Y. Huang, A new insight to the effect of calcium concentration on gelation process and physical properties of alginate films, J. Mater. Sci. 51 (12) (Jun. 2016) 5791–5801, https://doi.org/10.1007/s10853-016-9880-0.
[49] R. Abka-khajouei, L. Tounsi, N. Shahabi, A.K. Patel, S. Abdelkafi, P. Michaud, Structures, properties and applications of alginates, Mar. Drugs 20 (6) (May 2022) 364, https://doi.org/10.3390/md20060364.
[50] D. Shah, Y. Shah, R. Pradhan, Development and evaluation of controlled-release diltiazem HCl microparticles using cross-linked poly(vinyl alcohol), Drug Dev. Ind. Pharm. 23 (6) (Jan. 1997) 567–574, https://doi.org/10.3109/03639049709149821.
[51] B.C. Thanoo, M.C. Sunny, A. Jayakrishnan, Controlled release of oral drugs from cross-linked polyvinyl alcohol microspheres, J. Pharm. Pharmacol. 45 (1) (Apr. 2011) 16–20, https://doi.org/10.1111/j.2042-7158.1993.tb03671.x.
[52] J. Siepmann, N.A. Peppas, Higuchi equation: derivation, applications, use and misuse, Int. J. Pharm. 418 (1) (Oct. 2011) 6–12, https://doi.org/10.1016/j.ijpharm.2011.03.051.
[53] R.W. Korsmeyer, R. Gurny, E. Doelker, P. Buri, N.A. Peppas, Mechanisms of solute release from porous hydrophilic polymers, Int. J. Pharm. 15 (1) (May 1983) 25–35, https://doi.org/10.1016/0378-5173(83)90064-9.
[54] N.A. Peppas, Analysis of Fickian and non-Fickian drug release from polymers, Pharm. Acta Helv. 60 (4) (1985) 110–111.
[55] N.A. Peppas, J.J. Sahlin, A simple equation for the description of solute release. III. Coupling of diffusion and relaxation, Int. J. Pharm. 57 (2) (Dec. 1989) 169–172, https://doi.org/10.1016/0378-5173(89)90306-2.